

Functional Time Transformation Model with Applications to Digital Health

Rahul Ghosal¹, Marcos Matabuena², Sujit K. Ghosh³

¹ Department of Epidemiology and Biostatistics, University of South Carolina

² Department of Biostatistics, Harvard University, Boston, MA 02115, USA

³ Department of Statistics, North Carolina State University

July 1, 2024

Abstract

The advent of wearable and sensor technologies now leads to functional predictors which are intrinsically infinite dimensional. While the existing approaches for functional data and survival outcomes lean on the well-established Cox model, the proportional hazard (PH) assumption might not always be suitable in real-world applications. Motivated by physiological signals encountered in digital medicine, we develop a more general and flexible functional time-transformation model for estimating the conditional survival function with both functional and scalar covariates. A partially functional regression model is used to directly model the survival time on the covariates through an unknown monotone transformation and a known error distribution. We use Bernstein polynomials to model the monotone transformation function and the smooth functional coefficients. A sieve method of maximum likelihood is employed for estimation. Numerical simulations illustrate a satisfactory performance of the proposed method in estimation and inference. We demonstrate the application of the proposed model through two case studies involving wearable data i) Understanding the association between diurnal physical activity pattern and all-cause mortality based on accelerometer data from the National Health and Nutrition Examination Survey (NHANES) 2011-2014 and ii) Modelling Time-to-Hypoglycemia events in a cohort of diabetic patients based on distributional representation of continuous glucose monitoring (CGM) data. The results provide important epidemiological insights into the direct association between survival times and the physiological signals and also exhibit superior predictive performance compared to traditional summary based biomarkers in the CGM study.

Keywords: Functional Data Analysis; Time Transformation Model; Digital Health; CGM; NHANES; Accelerometer

1 Introduction

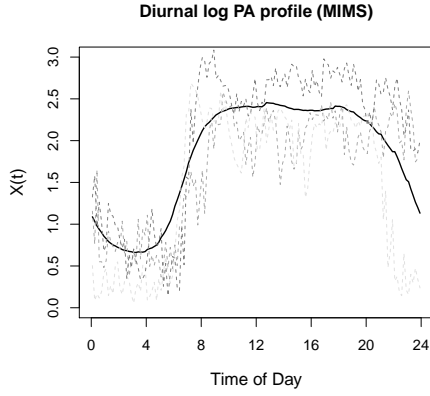
Advancements in wearable and sensor technology has resulted into collection of real-time, detailed physiological and behavioural signals tailored to individual users. These continuously collected observations can be treated as functional data (Ramsay and Silverman, 2005), which are intrinsically infinite dimensional, and can provide for a deeper understanding of the link between human behaviors and health and disease. Functional data analysis (FDA) refers to the branch of statistics analyzing data in the forms of curves or surfaces over a continuous index such as time or space. Functional data analysis has been applied across several areas in biosciences such as digital health (Cui et al., 2022; Ghosal and Maity, 2023; Ghosal et al., 2023; Matabuena and Petersen, 2023; Matabuena et al., 2023), genome-wide association studies (GWAS)(Wu and Müller, 2010; Huang et al., 2017), medical imaging (Zipunnikov et al., 2011, 2014; Li et al., 2021; Koner et al., 2024), ecology (Ikeda et al., 2008; Ghosal et al., 2020), intervention studies (Ghosal et al., 2023; Coffman et al., 2023) and many others.

In many biomedical and clinical studies, the objective is to enhance clinical decision-making and interpretation, by quantifying the association between a set of risk-factors and survival or time-to-event outcomes which are subject to censoring. Current biomedical and digital health studies often collect high dimensional physiological signals through wearable or sensor technologies such as physical activity (PA) data via accelerometer, blood glucose concentration using continuous glucose monitoring device (CGM), brain activity using EEG, among many others, which can be treated as Hilbert-space valued functional predictors. The existing approaches for functional data and survival outcomes primarily lean on the well-established Cox model (Gellar et al., 2015; Qu et al., 2016; Kong et al., 2018) and its extensions (Cui et al., 2021; Ghosal et al., 2023). However the proportional hazard (PH) assumption which forces the hazard ratio to be constant over time might not

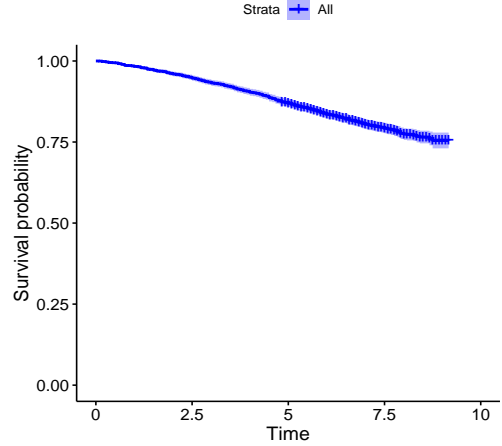
be suitable in many real-world applications and modelling the hazard itself can face lack of interpretability to the practitioners. Another recently proposed approach in the functional domain include the functional accelerated failure time (AFT) model (Liu et al., 2024).

1.1 Motivating Applications

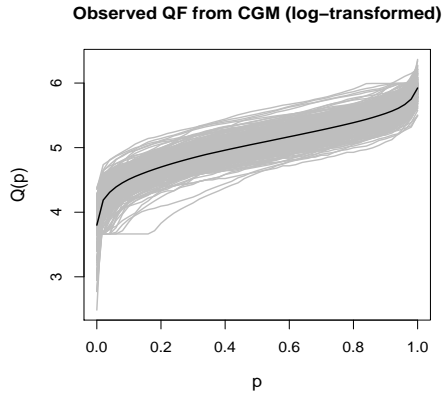
In this paper, as motivating applications, we consider two real case studies: (i) Modelling the survival time of older adults (aged 50 years or older) based on diurnal patterns of objectively measured physical activity data collected using accelerometer in the National Health and Nutrition Examination Survey (NHANES) 2011-2014 and other biological factors such as age, gender and body mass index (BMI). NHANES 2011-2014 reports individuals' acceleration in Monitor Independent Movement Summary (MIMS) unit (John et al., 2019). Figure 1a displays the average diurnal PA profile across all participants for log-transformed MIMS, along with the PA profile for three sample participants. Figure 1b displays the Kaplan-Meier plot for all-cause mortality through 2019 for the study participants. Previous research in NHANES exploring the relation between PA and all-cause mortality have primarily explored various summary measures of PA (Liu et al., 2016; Patel et al., 2019; Smirnova et al., 2020), or have used variants of functional Cox models for modelling the hazard of mortality (Cui et al., 2021) which have mostly been concentrated on the NHANES 2003-06 uni-axial accelerometer data. By directly modelling the survival time on the diurnal PA patterns, we aim to uncover the dynamic association between all-cause mortality and circadian rhythm of PA, which could be useful in designing time-of-day-specific PA interventions. (ii) We consider modelling time to 65 hypoglycemia events as an adverse outcome in a cohort of Type 1 diabetes mellitus (T1D) patients based on a compositional functional (Petersen and Müller, 2016) or distributional representation of continuous glucose monitoring (CGM) data collected at baseline.



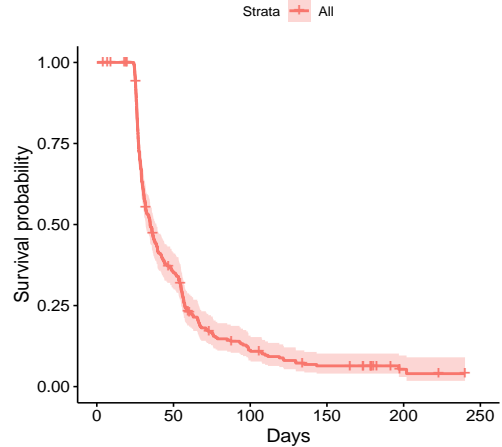
(a) Average diurnal PA (MIMS) profile (log-transformed) for NHANES 2011-2014 participants (solid), along with profiles for three randomly chosen participants (dashed).



(b) Kaplan-Meier marginal survival curve of all-cause mortality in the NHANES 2011-2014.



(c) Glucodensity profiles of all participants based on subject-specific quantile function representation along with the Wasserstein Barycenter of the profiles in the CGM study (solid).



(d) Kaplan-Meier plot for time to 65 hypoglycemia events in the CGM study.

Figure 1: Functional profiles and Kaplan Meier curves in the wearable applications.

Figure 1c displays the glucodensity profiles (Matabuena et al., 2021) of all participants and the Wasserstein Barycenter (Bigot et al., 2018) representing the average quantile function, based on the subject-specific quantile function representations (Ghosal et al., 2023; Matabuena and Petersen, 2023) of glucose-concentrations (log-transformed). The glucodensity based marker has been shown to demonstrate improved clinical sensitivity compared to the traditional markers like the time in range metric, HbA1c (Matabuena et al., 2021) in

diabetes and they provide more nuanced insight for assessing glucose metabolism. Figure 1d displays the Kaplan-Meier plot for the adverse event “time-to 65 hypoglycemia” for these study participants.

1.2 Background and Contributions

Time-transformation models (Cheng et al., 1995; Chen et al., 2002; Zeng and Lin, 2006) are a flexible and general class of survival models, which directly model the survival time based on a linear combination of covariates through an unknown monotone transformation $H(\cdot)$ and a known error distribution. The family of transformation models encompasses the popularly used Cox proportional hazards (PH) model, proportional odds (PO) model and accelerated failure time (AFT) models as special cases. Since, the survival time (or its monotone transformation) is modelled directly in the transformation models, the covariate effects are directly interpretable in terms of effect on the survival time or survival probability. There exists several estimation approaches in classical transformation models based on generalized estimating equations (GEE) (Chen et al., 2002), nonparametric maximum likelihood estimation (NPML) (Zeng and Lin, 2006, 2007), and sieve maximum likelihood estimation (McLain and Ghosh, 2013).

In this article, we develop a flexible partially functional time-transformation model for estimating the conditional survival function in the presence of both functional and scalar covariates. The proposed model is more general and include both the functional Cox and AFT model as special cases. We use Bernstein polynomials to model the monotone transformation and the smooth functional coefficients, and the sieve method of maximum likelihood (McLain and Ghosh, 2013; Ghosal et al., 2023) is employed for shape constrained and smooth estimation of the unknown functions. The resulting estimate of conditional survival function is smooth as opposed to the ones generally obtained in the functional cox model (Gellar et al., 2015), as is the estimate of the monotone transformation function

$H(\cdot)$, which facilitates interpretation of the effect of the covariates on survival time.

The key contributions of this paper are i) a partially functional time-transformation model relaxing the PH assumption and moving beyond functional Cox model ii) a computationally efficient sieve maximum likelihood estimation and incorporation of smoothness in the estimated monotone transformation and functional coefficients with Bernstein polynomials and iii) quantifying the association between functional and distributional representations of wearable data and survival time for two case studies; NHANES 2011-2014 data and the CGM study. In addition, we establish consistency of the proposed estimator under standard regularity conditions. Our empirical analyses using simulations illustrate a satisfactory finite-sample performance the proposed method. The two real case studies provide novel epidemiological insights into the association between the functional biomarkers and the corresponding survival time, which could be important for designing time-of-day or intensity-specific interventions.

The rest of this article is organized in the following way. The notations and the modeling framework are introduced in Section 2. The sieve maximum likelihood estimation method along with other methodological details are presented in Section 3. Section 4 reports the empirical analysis using simulation studies. Section 5 presents the Real data applications of the proposed method. We conclude with a discussion of the proposed method and some possible extensions of this work in Section 6.

2 Methodology

Let T_i be the survival time for subject i , and C_i the corresponding censoring time for $i = 1, \dots, n$. Let us denote $Y_i = \min(T_i, C_i)$ to be the observed survival time for subject i in the presence of right censoring, and $\Delta_i = I(T_i \leq C_i)$ is the event or censoring indicator for subject i . Suppose that we observe a random sample $(Y_i, \Delta_i, \mathbf{X}_i, X_{fi}(\cdot))$, $i = 1, \dots, n$,

having the same distribution as $(Y, \Delta, \mathbf{X}, X_f(\cdot))$. Conditionally on $(\mathbf{X}, X_f(\cdot))$, we assume that the survival time T is independent of the censoring time C . We observe the functional covariates $X_{fi}(\cdot)$ at the baseline and they are assumed to lie in a real separable Hilbert space, taken to be $L^2[0, 1]$ in this paper. The scalar baseline covariates are denoted as $\mathbf{X}_i = (X_{i1}, \dots, X_{ip})$. We further assume that the functional curves are observed on a dense and regular grid $S = \{s_1, \dots, s_m\} \subset \mathcal{S} = [0, 1]$, although this can be relaxed to accommodate more general scenarios, e.g., functions observed on irregular and sparse domain.

2.1 Functional Time Transformation Model

We posit the functional time transformation model (FTTM), where a monotone transformation of survival time T is additively modelled as linear function of the scalar covariates and a linear functional term of the functional covariate,

$$H(T) = -\{\boldsymbol{\beta}^T \mathbf{X} + \int_0^1 X_f(s)\beta(s)ds\} + \epsilon = -\left\{\sum_{j=1}^p \beta_j X_j + \int_0^1 X_f(s)\beta(s)ds\right\} + \epsilon. \quad (1)$$

Here ϵ is a random variable with a known distribution function $F_\epsilon(\cdot)$ and $H(\cdot)$ is an unknown monotone function. Throughout this paper, we assume $H(\cdot)$ to be monotone increasing, without loss of generality. The scalar coefficients β_j capture the expected decrease in the transformed survival time $H(T)$ for one unit increase in the covariate Z_j . Hence a positive β_j indicates a decrease in the expected survival time (since $H(\cdot)$ to be monotone increasing) with increase in X_j . Similarly, the functional coefficient $\beta(s)$ capture the expected decrease in the transformed survival time $H(T)$ for one unit increase in the functional covariate $X_f(s)$ at index s , keeping all the other covariates fixed.

The transformation model (1) reduces to proportional hazards model and a proportional odds model when ϵ follows the extreme-value and logistic distribution respectively. For $H(t) = \log(t)$, the transformation model reduces to the well known AFT model. When

the residual ϵ follows a Normal distribution, the model serves as an extension of the usual Box-Cox model. Hence, the transformation model (1) provides a generalization to several well known models used in survival and regression analysis. On the other hand, note that, in model (1) we are directly modelling the survival time of interest, rather than modelling the hazard or the odds of the event, and hence is more interpretable.

Based on model (1), we have $E(H(T)|\mathbf{X}, X_f(\cdot)) = -\{\boldsymbol{\beta}^T \mathbf{X} + \int_0^1 X_f(s)\beta(s)ds + \mu_\epsilon\}$, hence an approximation of expected survival time is given by $E(T|\mathbf{X}, X_f(\cdot)) \approx H^{-1}(-\{\boldsymbol{\beta}^T \mathbf{X} + \int_0^1 X_f(s)\beta(s)ds + \mu_\epsilon\})$. The sieve likelihood based estimation procedure, that will be used in this paper ensures a smooth and invertible $H(\cdot)$ function (McLain and Ghosh, 2013), where $H^{-1}(\cdot)$ is continuously differentiable and this aids in the interpretation of the coefficients, by associating them to the change in expected survival time $E(T|\mathbf{X}, X_f(\cdot))$. Let us denote the survival function of the error ϵ as \bar{F}_ϵ and the density as f_ϵ . The conditional survival function and conditional density of T based on model (1) is given by,

$$S_T(t|\mathbf{X}, X_f(\cdot)) = \bar{F}_\epsilon\{H(t) + \boldsymbol{\beta}^T \mathbf{X} + \int_0^1 X_f(s)\beta(s)ds\}, \quad (2)$$

$$\bar{F}_\epsilon^{-1}\{S_T(t|\mathbf{X}, X_f(\cdot))\} = H(t) + \boldsymbol{\beta}^T \mathbf{X} + \int_0^1 X_f(s)\beta(s)ds, \quad (3)$$

$$f_T(t|\mathbf{X}, X_f(\cdot)) = H'(t)f_\epsilon\{H(t) + \boldsymbol{\beta}^T \mathbf{X} + \int_0^1 X_f(s)\beta(s)ds\}. \quad (4)$$

The parameters $H(\cdot), \boldsymbol{\beta}, \beta(s)$ are identifiable if X is full rank and $Ke(K^{X_f}) = \{0\}$ (McLain and Ghosh, 2013; Scheipl and Greven, 2016), where K^{X_f} denotes the covariance operator of the functional process $X_f(\cdot)$ and $Ke(C)$ denotes the kernel or the null space of the operator C . For the error ϵ , we specifically consider the class of logarithmic error distribution (Chen et al., 2002) in this paper. The survival function of the error ϵ is given by $\bar{F}_\epsilon(t) = e^{-G(e^t)}$.

For the logarithmic error distribution class, we have,

$$G(t) = \frac{\log(1+rt)}{r} \text{ if } r > 0 \quad (5)$$

$$G(t) = t \text{ if } r = 0.$$

We get the extreme value and the logistic error distribution for $r = 0$ and $r = 1$, which leads to the well known PH and PO model respectively. Another possible choice for the error distribution are the class of Box-Cox type error distributions ([Zeng and Lin, 2006](#)), where $G(t) = \frac{(1+t)^\rho - 1}{\rho}$ if $\rho > 0$ and $G(t) = \log(1+t)$ if $\rho = 0$ respectively.

3 Estimation

We assume that F_ϵ is known and denote the unknown parameters as $\phi = (\boldsymbol{\beta}, \beta(\cdot), H(\cdot))$, with their true values being $\phi_0 = (\boldsymbol{\beta}_0, \beta_0(\cdot), H_0(\cdot))$. Further we assume that, $\tau = \inf\{t : P(T \wedge C > t) = 0\} < \infty$. We model both the unknown nonparametric functions $H(\cdot)$ and $\beta(s)$ in model (2) using univariate Bernstein basis polynomial expansions. The transformation function $H(\cdot)$ is modelled as,

$$H_{N_0}(t) = H_{N_0}(t; \tau, \boldsymbol{\gamma}) = \sum_{k=0}^{N_0} \gamma_k b_k(t/\tau, N_0). \quad (6)$$

Here $b_k(x, N) = \binom{N}{k} x^k (1-x)^{N-k}$, $0 \leq x \leq 1$. The number of basis polynomials depends on the order of the polynomial basis N_0 . Note that $b_k(x, N_0) \geq 0$ and $\sum_{k=0}^{N_0} b_k(x, N_0) = 1$. The unknown parameters of interest are then the basis coefficients $\boldsymbol{\gamma} = (\gamma_0, \gamma_1, \dots, \gamma_{N_0})^T$. Based on (3), the derivative of the transformation function $H'(t)$ is modelled as,

$$H'_{N_0}(t) = N_0 \sum_{k=0}^{N_0-1} (\gamma_{k+1} - \gamma_k) b_k(t/\tau, N_0 - 1) \times (1/\tau). \quad (7)$$

Let $H(\cdot) \in \mathcal{F}$, denote the space of continuous, bounded and increasing transformation functions considered in this paper. We define the constrained Bernstein polynomial sieve following [McLain and Ghosh \(2013\)](#); [Ghosal et al. \(2023\)](#) given by,

$$\mathcal{F}_N = \{H_N(t); M_l \leq \gamma_0 \leq \gamma_1 \leq, \dots, \leq \gamma_N \leq M_u\}, N = 1, 2, \dots \quad (8)$$

Our estimation procedure enforces the constraint $H_N(\cdot) \in \mathcal{F}_N \subset \mathcal{F}$. Let Γ_R^N denote the space of restricted parameters γ given by $\Gamma_R^N = \{\gamma \in \mathbb{R}^N \in; \gamma_0 \leq \gamma_1 \leq, \dots, \leq \gamma_N\}$. It can be easily seen that the sequence of function spaces \mathcal{F}_N is nested in \mathcal{F} and $\bigcup_{N=1}^{\infty} \mathcal{F}_N$ is dense in \mathcal{F} with respect to the sup-norm ([Wang and Ghosh, 2012](#)). This result along with the Bernstein-Weierstrass approximation theorem guarantee that $H_N(t)$ converges uniformly to $H_0(t)$ as $N \rightarrow \infty$, for $\gamma_k = H_0(K/N)$, for $k = 0, \dots, N$.

The functional coefficient $\beta(s)$ is modelled using Bernstein basis expansion as

$$\beta_{N_1}(s) = \sum_{k=0}^{N_1} \theta_k b_k(s, N_1). \quad (9)$$

Similarly based on Bernstein-Weierstrass approximation theorem, we know that $\beta_{N_1}(s)$ converges uniformly to $\beta(s)$ as $N_1 \rightarrow \infty$, for $\theta_k = \beta_0(K/N_1)$, for $k = 0, \dots, N_1$. Let $\mathbf{N} = (N_0, N_1)$, plugging in these basis expansions, the conditional survival and density functions of T is given by,

$$S_{\mathbf{N}}(t|\mathbf{X}, X_f(\cdot), \boldsymbol{\beta}, \boldsymbol{\gamma}, \boldsymbol{\theta}) = \bar{F}_{\epsilon}\{H_{N_0}(t) + \boldsymbol{\beta}^T \mathbf{X} + \sum_{k=0}^{N_1} \theta_k \int_0^1 X_f(s) b_k(s, N_1) ds\} \quad (10)$$

$$f_{\mathbf{N}}(t|\mathbf{X}, X_f(\cdot), \boldsymbol{\beta}, \boldsymbol{\gamma}, \boldsymbol{\theta}) = f_{\epsilon}\{H_{N_0}(t) + \boldsymbol{\beta}^T \mathbf{X} + \sum_{k=0}^{N_1} \theta_k \int_0^1 X_f(s) b_k(s, N_1) ds\} * H'_{N_0}(t) \quad (11)$$

The log-likelihood function for this right-censored scenario is given by,

$$l_n(\boldsymbol{\beta}, \boldsymbol{\gamma}, \boldsymbol{\theta} | \mathbb{X}, \mathbf{X}_f(\cdot), \mathbf{Y}) = \sum_{i=1}^n \Delta_i \log f_{\mathbf{N}}(Y_i | \mathbf{X}_i, X_{f_i}(\cdot), \boldsymbol{\beta}, \boldsymbol{\gamma}, \boldsymbol{\theta}) + (1 - \Delta_i) \log S_{\mathbf{N}}(Y_i | \mathbf{X}_i, X_{f_i}(\cdot), \boldsymbol{\beta}, \boldsymbol{\gamma}, \boldsymbol{\theta}). \quad (12)$$

The maximum likelihood estimate of the parameters $\boldsymbol{\psi} = (\boldsymbol{\beta}^T, \boldsymbol{\gamma}^T, \boldsymbol{\theta}^T)^T$ are given by

$$\hat{\boldsymbol{\psi}} = \underset{\boldsymbol{\psi} \in \Psi_R}{\operatorname{argmax}} l_n(\boldsymbol{\psi} | \mathbf{X}, X_f(\cdot), \mathbf{Y}), \Psi_R = \mathbb{R}^p \times \Gamma_R \times \mathbb{R}^{N_1}. \quad (13)$$

Once we have the estimates $\hat{\boldsymbol{\beta}}, \hat{\boldsymbol{\gamma}}$ and $\hat{\boldsymbol{\theta}}$, the estimates of the functions $H_0(t)$ and $\beta(s)$ are given by $\hat{H}_0(t) = \sum_{k=0}^{N_0} \hat{\gamma}_k b_k(t/\tau, N_0)$ and $\hat{\beta}(s) = \sum_{k=0}^{N_1} \hat{\theta}_k b_k(s, N_1)$, respectively. Note that the monotonicity restrictions on $\boldsymbol{\gamma}$ given by $\gamma_0 \leq \gamma_1 \leq \dots \leq \gamma_N$, can be enforced by reparametrizing $\eta_0 = \gamma_0$ and $\exp(\eta_k) = \gamma_k - \gamma_{k-1}$, for $k = 1, \dots, N$.

3.1 Variance Estimation and Inference

The variance covariance matrix of the maximum likelihood estimates $\hat{\boldsymbol{\psi}}$ are estimated based on the observed Fischer information matrix at the MLE. In particular, the observed Fischer information matrix is given by $\mathcal{J}(\hat{\boldsymbol{\psi}}) = -\frac{\partial^2 l_n(\boldsymbol{\psi} | \mathbf{X}, X_f(\cdot), \mathbf{Y})}{\partial \boldsymbol{\psi} \partial \boldsymbol{\psi}^T} \Big|_{\boldsymbol{\psi}=\hat{\boldsymbol{\psi}}}$. The estimates of the asymptotic variance covariance matrix of the estimates then are given by $\hat{V}(\hat{\boldsymbol{\psi}}) = (\mathcal{J}(\hat{\boldsymbol{\psi}}))^{-1}$. Once the estimates of $\hat{\boldsymbol{\beta}}, \hat{H}_0(t)$ and $\hat{\beta}(s)$ are obtained, we define the Wald confidence intervals (point-wise for the functional parameters) as estimate $\pm 1.96^*$ se, based on the estimates and their estimated standard errors. Theoretical details regarding consistency of the estimators are provided in Appendix A of the Supplementary Material, under standard regularity conditions, following the results in [McLain and Ghosh \(2013\)](#).

3.2 Choice of Tuning Parameters

The number of basis functions N_0 and N_1 are a function of sample size n and are chosen in a data-driven way. Asymptotically, for both of these parameters, we have $N_j = O(n^{k_j})$, $k_j \in (0, 1)$. The parameter N_0 controls the smoothness of the transformation function H . The parameter of N_1 controls the smoothness of the functional coefficient $\beta(s)$. In this paper, we follow a truncated basis approach, by restricting the number of Bernstein polynomial bases to incorporate smoothness (Ramsay and Silverman, 2005; Fan et al., 2015). In finite sample size, we use the Akaike information criterion (AIC) defined below to choose N_0, N_1 using a grid-search providing the empirically minimum AIC,

$$AIC(\mathbf{N}) = AIC(N_0, N_1) = -2l_n(\boldsymbol{\beta}, \boldsymbol{\gamma}, \boldsymbol{\theta} | \mathbf{X}, X_f(\cdot), \mathbf{Y}) + 2(p + N_0 + N_1 + 1). \quad (14)$$

4 Simulation Study

In this Section, we investigate the performance of the proposed estimation and inference method for the proposed FTTM via simulations. To this end, we consider the following data generating scenarios.

4.1 Data Generating Scenarios

Scenario A1: Functional Proportional Hazard Model

We generate the survival times following the functional Cox model with the PH structure,

$$\log \lambda_i(t | \mathbf{X}_i, X_{fi}(\cdot)) = \log \lambda_0(t) + X_{i1} \beta_1 + X_{i2} \beta_2 + \int_0^1 X_{fi}(s) \beta(s) ds, i = 1, 2, \dots, n.$$

The baseline survival time follows an exponential distribution with rate e^{β_0} , hence the baseline hazard is taken as $\lambda_0(t) = e^{\beta_0} = 0.2$. The scalar covariates X_{i1}, X_{i2} are independently

generated from a Bernoulli (0.5) and a standard Normal distribution. The functional predictors $X_{fi}(\cdot)$ are independently generated as $X_{fi}(s) = \sum_{k=1}^{10} \psi_{ik} \phi_k(s)$, where $\phi_k(s)$ are orthogonal basis polynomials (of degree $k - 1$) and ψ_{ik} are mean zero and independent Normally distributed scores with variance $\sigma_k^2 = 4(10 - k + 1)$. They are observed on a dense and regular grid of length $m = 101$ on $\mathcal{S} = [0, 1]$. The scalar and the functional coefficients are taken to be $\boldsymbol{\beta} = (-0.5, 0.4)$, $\beta(s) = \cos(\pi s)$ respectively. Censoring times are independently generated from an exponential distribution with mean 20, which results into a censoring rate of approximately 26%. We take τ to be the nearest integer, larger than the maximum observed time. As mentioned in Section 2.1 this is a special case of the FTTM with the extreme value error distribution, specified by $r = 0$ in our error model (3) and $H(t) = \log(0.2t)$. We consider three sample sizes $n \in \{100, 300, 500\}$ and 100 Monte-Carlo (M.C) replications from the above data generating scenario.

Scenario A2: Functional Proportional Odds Model

We generate survival times from the FTTM,

$$S_T(t|\mathbf{X}, X_f(\cdot)) = \bar{F}_\epsilon \{ H(t) + X_{i1}\beta_1 + X_{i2}\beta_2 + \int_0^1 X_f(s)\beta(s)ds \},$$

where we assume ϵ follows a logistic distribution with survival function $\bar{F}_\epsilon(t) = \frac{1}{1+e^t}$ and $H(t) = \log(t^2)$. As mentioned in Section 2.1, this is a special case of the FTTM with the logistic error distribution, specified by $r = 1$ in our error model (3) and leads to a PO model, with $\text{logit}\{F(t|\mathbf{X}, X_f(\cdot))\} = H(t) + X_{i1}\beta_1 + X_{i2}\beta_2 + \int_0^1 X_f(s)\beta(s)ds$. The scalar and the functional covariates are generated as in scenario A1. The scalar and the functional coefficients are taken to be $\boldsymbol{\beta} = (-0.8, 1.6)$, $\beta(s) = 2\sin(\pi s)$ respectively. Censoring times are independently generated from an exponential distribution with mean 5, which results into a censoring rate of approximately 30%. We again consider three sample sizes $n \in$

$\{100, 300, 500\}$ and 100 Monte- Carlo (M.C) replications from the above data generating scenario.

4.2 Simulation Results

Performance under scenario A1

We apply the proposed FTTM to estimate the scalar coefficients (β_1, β_2) , the functional coefficient functions $\beta(s)$ and the transformation function $H(t)$. The extreme value distribution with $r = 0$ corresponding to equation (3) is used as the error distribution. The optimal order of BP basis N_0, N_1 are chosen using a grid-search over $N_0 \in \{4, 7, 10, 13\}$ and $N_1 \in \{3, 5, 7, 9\}$, providing the minimum AIC value in (12). We also fit the linear functional cox model (Gellar et al., 2015) for comparison purpose, which is the true generating model in this case and avoids smooth semi-parametric estimation of $H(t)$. The distribution of the estimated scalar parameters from both the approach are displayed in Figure 2, for sample size $n = 300$. The estimates from the FTTM can be noticed to be slightly more biased compared to the oracle functional Cox model.

The estimates of the functional coefficients $\beta(s)$ and the transformation function $H(t)$ from the FTTM averaged over 100 M.C replications are shown in Figure 3, for sample size $n = 300$. The average estimated coefficient function for $\beta(s)$ from the linear functional cox model is also included for comparison. We observe that the true functional coefficient $\beta(s)$ are estimated accurately by both the FTTM and the functional Cox model, although the FTTM exhibits a slightly higher point-wise bias. The transformation function $H(t)$ is also closely approximated by the M.C mean estimate from the FTTM, except for very small values of t , where a positive bias can be noticed.

We report the Monte Carlo (M.C) mean square error (MSE) of the estimated scalar parameters and the mean integrated squared error ($MISE = \frac{1}{M} \sum_{j=1}^M \int_0^1 \{\hat{\beta}^j(s) - \beta(s)\}^2 ds$)

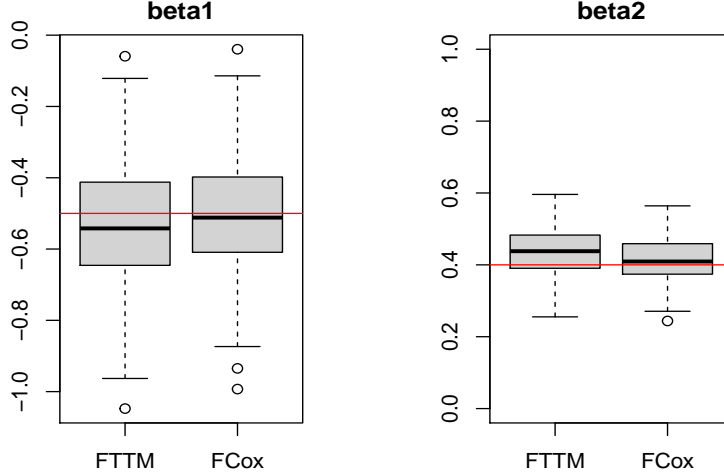


Figure 2: Boxplots of $\hat{\beta}_1, \hat{\beta}_2$ from the FTTM and a linear functional Cox model (FCox), scenario A1, $n=300$. The red solid line indicates the true value of the parameters.

of the estimates of the functional parameter ($\beta(s)$) for both the FTTM and the functional Cox model in Table 1 across all three sample sizes. For the FTTM we also report the MISE of the estimated transformation function $H(\cdot)$ obtained over a grid of time-points.

Table 1: Monte Carlo mean squared error of the estimated scalar and functional parameters from the functional time transformation model (FTTM) and the oracle functional Cox model, under Scenario A1. The Cox model performance is given in the parenthesis.

| Sample Size | MSE β_1 | MSE β_2 | MISE $\beta(s)$ | MISE $H(t)$ |
|-------------|---------------|----------------|-----------------|-------------|
| n=100 | 0.110 (0.082) | 0.025 (0.0171) | 0.448 (0.142) | 0.211 |
| n=300 | 0.030 (0.025) | 0.006 (0.004) | 0.124 (0.045) | 0.149 |
| n=500 | 0.016 (0.013) | 0.003 (0.003) | 0.067 (0.030) | 0.152 |

The proposed estimation method for FTTM does a satisfactory job in estimating the true scalar and functional parameters, with accuracy improving with increasing sample size. The functional Cox model is the oracle model in this scenario, which avoids estimation of H (an additional parameter estimated in our FTTM) by using partial log-likelihood (Gellar et al., 2014), and produces a better performance which is expected, on account of being less biased compared to the FTTM in this case.

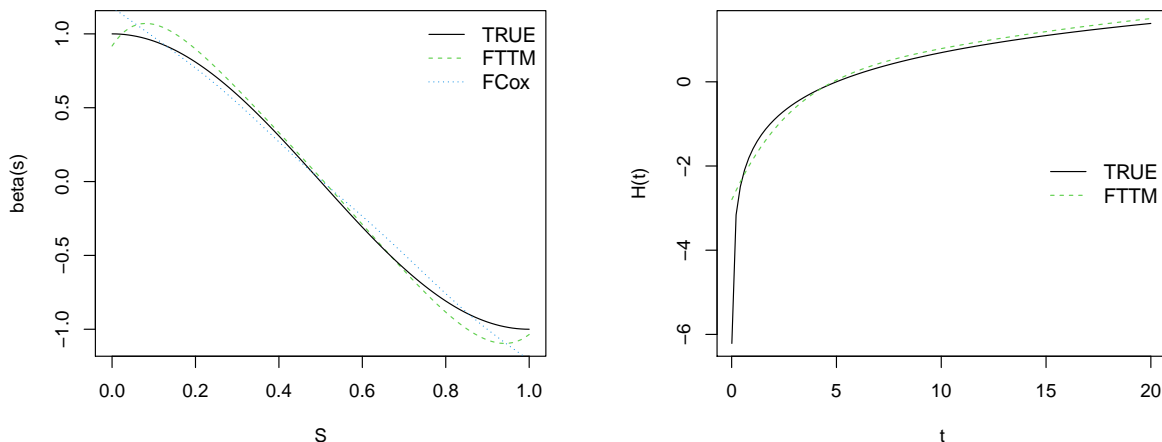


Figure 3: Left: True functional effect $\beta(s)$ (solid) and estimated $\hat{\beta}(s)$ averaged over 100 M.C replications from the FTTM (dashed) and functional Cox model (dotted), scenario A1, $n = 300$. Right: True $H(t)$ (solid) and estimated $\hat{H}(t)$ from the FTTM averaged over 100 M.C replications (dashed).

We also explore the coverage of the Wald confidence intervals developed in Section 2.3 based on the model based standard errors, for the scalar and functional coefficients. We set the the tuning parameter combination to be $N_0 = 13, N_1 = 3$ for this analysis, which was the best performing parameters (providing the lowest AIC) across the 100 M.C replications while estimation. The estimated coverage from 95% Wald confidence intervals across 100 Monte Carlo replications are presented in Supplementary Table S1. We report the average point-wise coverage over S for the functional coefficient $\beta(s)$. The estimated coverage can be observed to be close to the nominal level of 0.95 for both the scalar and functional parameters indicating a satisfactory performance of the proposed method.

Performance under scenario A2

We again apply the proposed FTTM to estimate the model parameters. The error distribution used in this case is the logistic distribution with $r = 1$ corresponding to equation (3). The optimal order of BP basis N_0, N_1 are chosen using a grid-search providing the

minimum AIC value as in the previous scenario. As competing models, We fit i) the linear functional cox model (termed as FCox), which will be misspecified in this scenario, and ii) a functional extension of the semiparametric proportional odds model proposed in Eriksson et al. (2015). In this approach (termed as FPO), we use the functional principal component (FPC) scores of the functional covariate $X(s)$ explaining more than 95% variability, as additional scalar predictors. The distribution of the estimated scalar parameters from both the approach are displayed in Figure 4, for sample size $n = 300$. The estimates from the FTTM can be noticed to accurately capture the true parameters, where as both FCox and FPO lead to high biases.

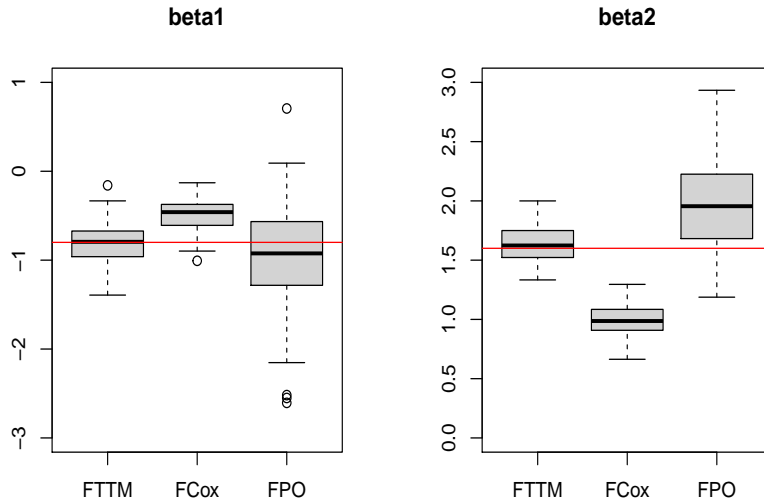


Figure 4: Boxplots of $\hat{\beta}_1, \hat{\beta}_2$ from the FTTM, a linear functional Cox model (FCox), and the FPO model under scenario A2, $n=300$. The red solid line indicates the true value of the parameters.

The M.C mean estimates of the functional coefficients $\beta(s)$ and the transformation function $H(t)$ from the FTTM are shown in Figure 5, for sample size $n = 300$. The average estimated coefficient function for $\beta(s)$ from the FCox and FPO is also included for comparison. We observe that the true functional coefficient $\beta(s)$ are estimated accurately by the FTTM, whereas the FCox and FPO estimate exhibit a high bias. Moreover, the

FPO estimate is highly non-smooth, whereas the FTTM produces a smooth estimate of the functional coefficient due to the truncated basis selection. The transformation function $H(t)$ is again closely estimated from the FTTM, except for very small values of t .

The Monte Carlo (M.C) mean square error (MSE) of the estimated scalar and functional parameters for the FTTM, FCox, and the FPO model are reported in in Table 2 across all three sample sizes. The MISE of the estimated transformation function $H(\cdot)$ is also reported for FTTM. A satisfactory performance of FTTM can be observed for all the parameters especially for larger sample sizes.

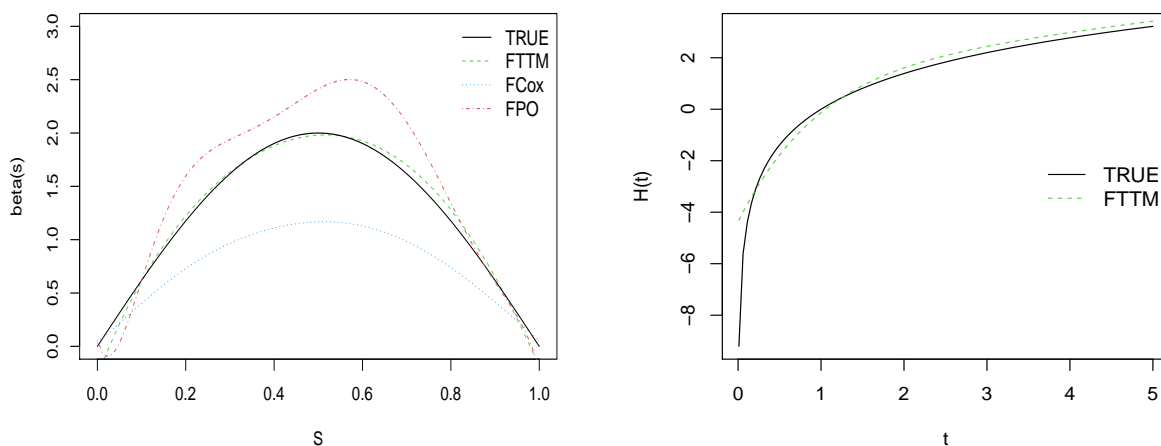


Figure 5: Left: True functional effect $\beta(s)$ (solid) and estimated $\hat{\beta}(s)$ averaged over 100 M.C replications from the FTTM (dashed), FCox (dotted), FPO (dashed-dotted), under scenario A2, $n = 300$. Right: True $H(t)$ (solid) and estimated $\hat{H}(t)$ from the FTTM averaged over 100 M.C replications (dashed).

Table 2: Monte Carlo mean squared error of the estimated scalar and functional parameters from the functional time transformation model (FTTM), FCox and FPO model under scenario A2. The FCox and FPO model performances are given in the parenthesis.

| Sample Size | MSE β_1 | MSE β_2 | MISE $\beta(s)$ | MISE $H(t)$ |
|-------------|---------------------|---------------------|---------------------|-------------|
| n=100 | 0.251 (0.188,0.889) | 0.114 (0.320,0.506) | 0.819 (0.554,9.360) | 0.568 |
| n=300 | 0.049 (0.125,0.415) | 0.025 (0.383,0.280) | 0.212 (0.409,3.87) | 0.375 |
| n=500 | 0.028 (0.109,0.383) | 0.012 (0.421,0.208) | 0.111 (0.379,2.92) | 0.378 |

Overall, the proposed estimation method for FTTM clearly outperforms the FCox model, on average producing 2.4, 17.7 times smaller MSE for the scalar parameters β_1, β_2 , and 2 times smaller MISE for the functional parameter $\beta(s)$. Similarly, compared to the FPO model, the FTTM on average produces 8.6, 11 times smaller MSE for the scalar parameters β_1, β_2 , and 18.7 times smaller MISE for the functional parameter $\beta(s)$. The improvement in the performance is particularly pronounced for the higher sample sizes. As in scenario A1, we report the estimated coverage of the parameters from 95% Wald confidence intervals across 100 Monte Carlo replications in Supplementary Table S2, for the tuning parameter choice $N_0 = 13, N_1 = 3$. The estimated coverage is observed to be close to the nominal level of 0.95 for both the scalar and functional parameters.

5 Real Data Application

5.1 Modelling All-cause Mortality in NHANES 2011-2014

In this study, we are interested in quantifying the association between diurnal patterns of objectively measured physical activity and all-cause mortality among the older adult population (aged 50 years or older) in USA. We apply the proposed FTTM to physical activity data collected via accelerometer from the National Health and Nutrition Examination Survey (NHANES) 2011-2014 and all-cause mortality data through 2019 while adjusting for age, gender and body mass index (BMI) at baseline. The NHANES provides a broad range of descriptive health and nutrition statistics and is a nationally representative sample of the non-institutionalized US population. In the NHANES 2011-2014, accelerometry data was collected using the ActiGraph GT3X+ accelerometer worn on the wrist (manufactured by ActiGraph of Pensacola, FL). Participants were instructed to wear the activity monitor continuously for seven days, removing it on the morning of the 9th day. Our analysis focuses on the minute-level accelerometer data from 2011 to 2014, which was made available

in 2021. This data reports individuals' acceleration in Monitor Independent Movement Summary (MIMS) units, an open source device-independent metric for summarizing movement activity (John et al., 2019). It is possible to link NHANES 2011-2014 data to the National Death Index (NDI) (Leroux et al., 2019) for collecting mortality information. For this purpose, we use the latest (December 31, 2019) mortality information from NDI (<https://www.cdc.gov/nchs/data-linkage/mortality-public.htm>) to define our survival outcome.

A total of 3032 adults aged 50 years or older (with physical activity monitoring available at least ten hours per day for at least four days) with available mortality and covariate (age, gender, and BMI) information were included in our analysis. The descriptive statistics of the sample is reported in supplementary Table S3. We denote the log-transformed MIMS as $X_{ij}(s)$, $s \in [0, 1440]$, which represent the log-transformed MIMS ($A \rightarrow \log(1 + A)$) for the individual i on the day j at time s , $i = 1, \dots, n$, and $j = 1, \dots, n_i$. The diurnal average functional curve $X_i(s) = \frac{1}{n_i} \sum_{j=1}^{n_i} X_{ij}(s)$ is considered as the functional covariate of interest. The diurnal curves $X_i(s)$ are further aggregated into 10 minutes epochs to make the PA profiles smoother for each subject. Survival time is calculated in years from the end of accelerometer wear, with all subjects being censored on December 31, 2019. Among the 3032 study participants considered at the baseline, 582 (19.2%) were deceased by the end of the study. The mean follow-up time of the subjects is 6.4 years. Figure 6 left panel displays the average diurnal PA profile of subjects for the deceased group and the survivors. The deceased group can be observed to have lower PA compared to the survivors particularly during the day-time.

FTTM for modelling all-cause mortality

We fit the following FTTM developed in this article, to directly model all-cause survival based on the diurnal PA profile and age, gender ($G_i = 1$ for Female) and BMI.

$$H(T_i) = -\{\beta_1 Age_i + \beta_2 G_i + \beta_3 BMI_i + \int_0^1 X_i(s)\beta(s)ds\} + \epsilon_i. \quad (15)$$

We assume ϵ is coming from the class of logarithmic error distribution described in error model (3), where the distribution function $F_\epsilon(\cdot)$ is known for a fixed value of r . Instead of fixing the value of r , we try several candidate models varying $r \in \{0, 0.05, 0.1, \dots, 0.1\}$, and chose the one which produces the minimum AIC proposed in Section 2.4. Note that this includes the Cox model (PH) and the PO model as special cases for $r = 0, 1$ respectively. The tuning parameters $N_0 \in \{6, 9, 12, 15, 18\}$ and $N_1 \in \{2, 3, 4, 5\}$ are also varied to control the smoothness of the transformation function and the functional coefficient. The optimal combination of N_0, N_1, r chosen using the proposed AIC is given by $N_0 = 9, N_1 = 4, r = 0.35$ producing an AIC of 4715.1.

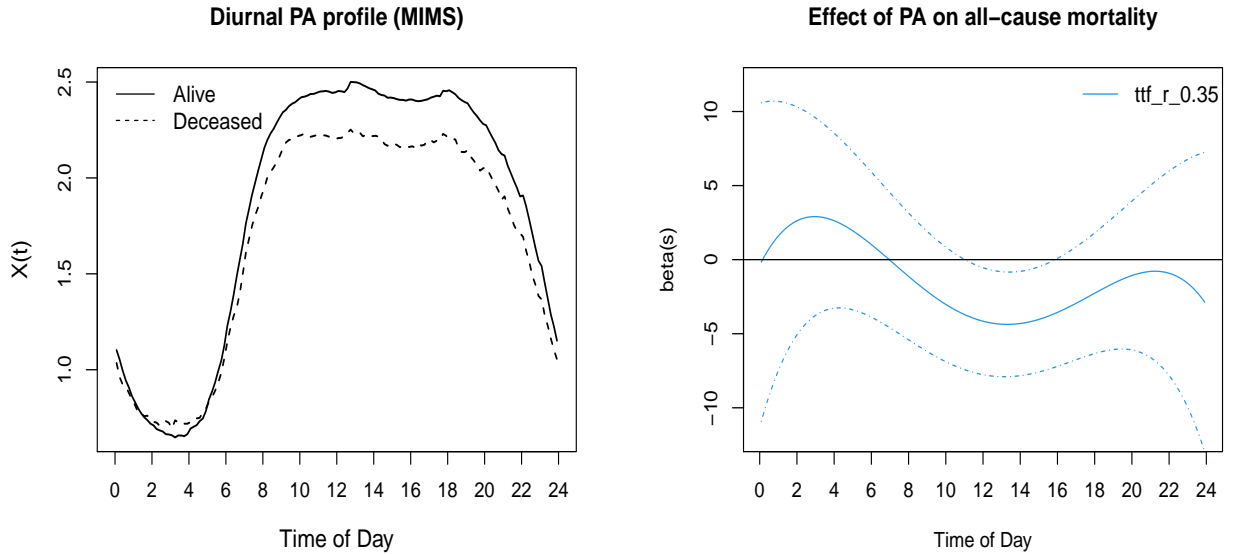


Figure 6: Left: Average diurnal PA profile (log-MIMS) of subjects for the deceased group (dashed) and the survivors (solid) in the NHANES application. Right: Estimated dynamic effect $\hat{\beta}(s)$ (solid) from the FTTM capturing the effect of diurnal PA on all-cause mortality and it's associated 95% point-wise confidence interval (dashed and dotted).

The estimated functional coefficient $\hat{\beta}(s)$ along with the corresponding 95% point-wise

confidence interval is displayed in Figure 6 right panel. The estimated effect $\hat{\beta}(s)$ is negative during the daytime 11 am - 4pm, indicating a higher diurnal PA during these times of day is associated with a higher survival time (or it's increasing transformation) and a higher survival probability following model (13). The estimated scalar coefficients and their associated 95% confidence intervals are reported in Supplementary Table S4, where we observe a higher age to be associated ($\hat{\beta}_1 = 0.8$) with a reduced survival probability.

We display the predicted survival probability plots $\hat{S}_T(t|\mathbf{X}, X(\cdot)) = \bar{F}_{\epsilon, r=0.35}\{\hat{H}(t) + \hat{\beta}_1 Age_i + \hat{\beta}_2 G_i + \hat{\beta}_3 BMI_i + \int_0^1 X_i(s)\hat{\beta}(s)ds\}$ in Supplementary Figure S2 for male and female subjects with age = 66 years at baseline and having BMI= 30.06 Kg/m^2 , using the mean value of age, BMI at baseline and the diurnal PA curve $X(s)$ belonging to either of high, average, or low group. The ‘‘High’’, ‘‘average’’ and ‘‘low’’ group was defined as having $X(s) = \bar{X}(s) + 0.5$, $X(s) = \bar{X}(s)$, and $X(s) = \bar{X}(s) - 0.5$ at baseline respectively for illustrative purposes, where $\bar{X}(s)$ denotes the sample average. We notice that higher PA leads to a better survival for both the genders, illustrating a protective effect of PA.

Graphical check of model fit

Note that since the optimal r (0.35) chosen by the AIC is non-zero, this indicates a departure from the PH model. To validate our model, we propose a goodness-of-fit check based on the fitted survival function, which is similar to a graphical check using Cox-Snell residuals. If the model is correctly specified, $-\log\{\hat{S}_T(T_i|\mathbf{X}_i, X_i(\cdot))\} \sim exp(1)$, hence the observations $U_i = -\log\{\hat{S}_T(Y_i|\mathbf{X}_i, X_i(\cdot))\}$ should behave like a censored sample from an exponential distribution with mean 1. This can be graphically checked by using the Nelson-Allen estimator based on fitted U_i 's, $i = 1, \dots, n$, which we term as FTTM pseudo residuals. If the fit is good, we can expect $\hat{\Lambda}(U_i) = U_i$, for an unit mean exponential distribution. The estimated cumulative hazard function of U_i s are shown in Supplementary Figure S2, which closely follows the 45 degree line $\Lambda(U_i) = U_i$. Hence, a satisfactory model fit can be

concluded based on the FTTM analysis.

5.2 Modelling Time to Multiple Hypoglycemia events in CGM Study

In this application, the high dimensional physiological signal we consider is continuous glucose monitoring (CGM) data collected by the Juvenile Diabetes Research Foundation (JDRF) CGM study group (Group, 2009) in a cohort of Type 1 diabetes mellitus (T1D) patients. This was the first landmark randomized clinical trial (RCT) investigating the efficacy and safety of CGM. Continuous Glucose Monitoring (CGM) plays an important role in diabetes management and can help in improving glycemic control (Burge et al., 2008; Allen et al., 2009). The adverse event, we consider in this study is Hypoglycemia (van Beers and DeVries, 2016; Hermanns et al., 2019), which arises when blood sugar (glucose) level is lower than the standard range. Although prior research over the last decade has demonstrated that real-time continuous glucose monitoring improves glycemic control in terms of lowering glycated hemoglobin levels (HbA1c), such significant effect has not been established for mild or severe hypoglycemia (van Beers and DeVries, 2016).

Traditionally CGM data have been analyzed using summary level metrics such as the mean (Battelino et al., 2023), which can result in substantial loss of information. As an example, consider two individuals with similar mean CGM, but with very different profiles, one stable around the mean and another with long excursions into the hyper and hypo-glycemic ranges. These two individuals would require different interventions, but would be hard to distinguish based on mean CGM or HbA1c (average blood sugar (glucose) over past three months), the primary biomarker used for diabetes. Hence, in this article, we propose to use distributional representation of CGM data at baseline (spanning a 10 day period) via subject-specific quantile function $Q_i(p)$ (Ghosal et al., 2023) as a

functional predictor which is directly related to glucodensities introduced in [Matabuena et al. \(2021\)](#). Specifically, We focus on the empirical quantile function of each participant’s log-transformed glucose measurements in this application. This is defined as $\hat{Q}_i(p)$, where $p \in [0, 1]$ and this can be obtained as the generalized inverse of the empirical cumulative distribution function (CDF) associated with the participant’s glucose levels. The empirical CDF, $\hat{F}_i(a)$, captures the proportion of glucose measurements that do not exceed a certain level a , is given by $\hat{F}_i(a) = \frac{1}{n_i} \sum_{j=1}^{n_i} \mathbf{1}\{G_{ij} \leq a\}$, where $G_{ij}, j = 1, 2, \dots, n_i$ are the glucose values recorded for the i -th participant.

In our analysis, we consider a subsample of 296 subjects from the JDRF study, with available age, Gender, baseline HbA1c and baseline CGM information. The descriptive statistics of the sample is presented in Supplementary Table S5. We define episodes of hypoglycemia as a plasma glucose of ≤ 70 mg/dl. We define our survival outcome as time to 65 hypoglycemic events over a maximum follow up period of 240 days which correspond to a subject having mild ([Östenson et al., 2014](#)) hypoglycemia (1-2 events per patient per week). In our sample of 296 subjects, 260 (87.8%) subjects had the adverse event (65 hypoglycemic episodes) by the end of the followup, with the mean follow-up time being 51.2 days. Figure 7 left panel displays the average quantile function (Wasserstein Barrycenter) $Q_G(p), G = 1, 2$ of log-transformed glucose values for two groups, subjects who experienced the adverse event (“Events”) and those who didn’t (“No events”). The events group can be observed to have a lower minimal and maximal quantiles compared to the no events group. We are interested in directly modelling the survival time of this adverse event based on the glucodensity representation $Q_i(p)$ while adjusting for age, Gender, and also investigate whether glucodensity can provide an improved predictive capacity for assessing the risk of hypoglycemia compared to traditional glucose biomarkers such as hemoglobin A1c (HbA1c).

FTTM for modelling time to multiple Hypoglycemia

We fit the FTTM developed in this article, to directly model the survival time T_i of this adverse event based on the glucodensity representation $Q_i(p)$ and adjusting for age, Gender ($(G_i = 1$ for Male)).

$$H(T_i) = -\{\beta_1 Age_i + \beta_2 G_i + \int_0^1 Q_i(p)\beta(p)dp\} + \epsilon_i. \quad (16)$$

The error ϵ is again assumed to be coming from the class of logarithmic error distribution described in error model (3), where the distribution function $F_\epsilon(\cdot)$ is known for a fixed value of r . We try several candidate models varying $r \in \{0, 0.2, 0.4, \dots, 4\}$, and chose the one which produces the minimum AIC. The tuning parameters $N_0 \in \{6, 9, 12, 15, 18, 21\}$ and $N_1 \in \{2, 3, 4, 5, 6\}$ are also varied to control the smoothness of the transformation function and the functional coefficient. The optimal combination of N_0, N_1, r chosen using the proposed AIC is given by $N_0 = 21, N_1 = 4, r = 4$ producing an AIC of 2272.3. In comparison the optimal Cox model ($r = 0$) had AIC 2359.4 and the optimal PO model ($r = 1$) had AIC 2314.8. A high $r = 4$ value in this case indicates the covariate effects to be decreasing over time (Zeng and Lin, 2006).

The estimated coefficient $\hat{\beta}(p)$ along with the corresponding 95% point-wise confidence interval is displayed in Figure 7 right panel. The estimated effect $\hat{\beta}(p)$ is found to capture a contrast between CGM values at higher quantile range $p \in [0.7, 0.9]$ and CGM values at very low quantile range $p \in [0, 0.1]$. A high negative value of this contrast (indicating a higher maximal CGM levels and smaller minimal CGM levels) is found to be associated with a higher survival probability for time to 65 Hypoglycemia. We report the estimated scalar coefficients and their associated 95% confidence intervals in Supplementary Table S6, which were not found to be significant after adjusting for the distributional CGM profile.

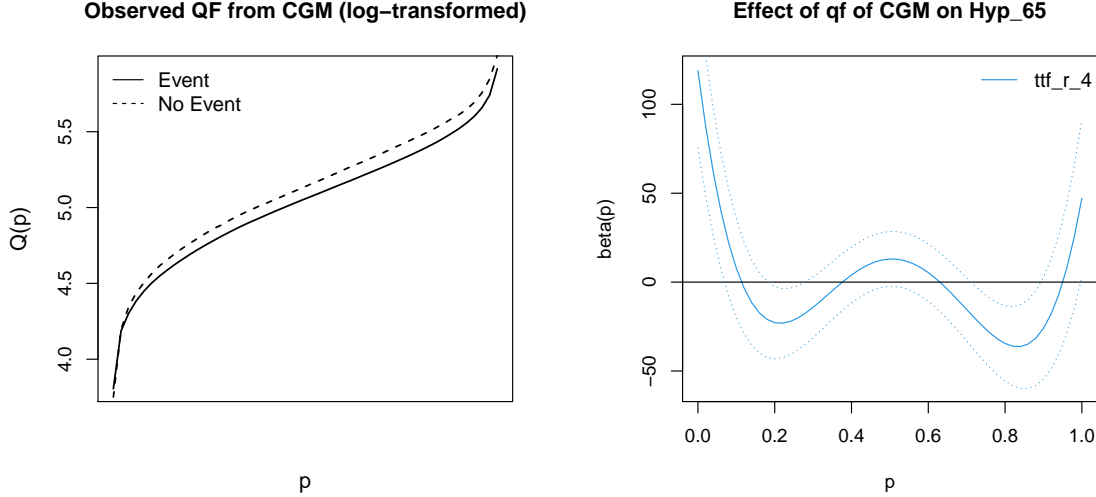


Figure 7: Left: Average quantile function of log-transformed CGM for the “Events” group” (solid) and “No events” group (dashed) in the CGM application. Right: Estimated dynamic effect $\hat{\beta}(p)$ (solid) from the FTTM capturing the distributional effect of CGM on time to 65 Hypoglycemia events and it’s associated 95% point-wise confidence interval (dashed and dotted).

Graphical check of model fit

We again use a graphical check based on the fitted survival function, using the FTTM pseudo residuals $U_i = -\log\{\hat{S}_T(Y_i|\mathbf{X}_i, Q_i(\cdot))\}$ for $r = 4$. The estimated cumulative hazard function and the associated 95% confidence interval are shown in Supplementary Figure S3, which are close to the 45 degree line, $\Lambda(U_i) = U_i$. Hence, a satisfactory model fit can be concluded based on our analysis.

Predictive comparison with traditional glucose biomarkers

We compare the predictive performance of the FTTM (14) for $r = 4$ using CGM based glucodensity $Q_i(p)$ with i) a Cox model using traditional glucose biomarker HbA1c, while adjusting for age and gender and ii) A functional cox model (Gellar et al., 2015) employing penalized partial likelihood (PPL) based estimation, with $Q_i(p)$ as the functional predictor, and adjusting for age and gender. We obtain the average 10-fold cross-validated Harrell’s

C-index (concordance index) (Harrell Jr et al., 1996) for all the models. The cross-validated C-index is calculated to be 0.641 for the proposed FTTM, 0.56 with HbA1c based Cox model and 0.626 for the distributional Cox model with $Q_i(p)$. This illustrate, with glucodensity based FTTM we get an 14.5% improvement in predictive capacity of the model, compared to the traditional biomarker HbA1c used in a Cox model. The proposed FTTM approach, also exhibit a 2.4% improvement over the functional Cox model with $Q_i(p)$.

Our results in this section highlight the usefulness of the proposed FTTM in survival analysis with infinite-dimensional functional covariates.

6 Discussion

In this paper we have developed a functional time-transformation model (FTTM) for estimating the conditional survival function in the presence of both functional and scalar covariates. This provides a flexible way to directly model a monotone transformation of survival time in clinical and epidemiological studies based on high dimensional physiological signals which can be treated as functional covariates. We have used Bernstein polynomials to model the monotone transformation and the smooth functional coefficients, and have employed a sieve method of maximum likelihood for estimation. Since we perform maximum likelihood estimation, we are able to obtain asymptotic standard errors and the point-wise confidence intervals of the model coefficients using the observed information matrix under standard regularity conditions. Theoretical results regarding consistency of the estimators are also established.

Numerical analysis using simulations illustrate the satisfactory finite-sample performance of the proposed estimation method for FTTM in accurately estimating the scalar, functional coefficients and the monotone transformation function. In the NHANES 2011-2014 application, the proposed method demonstrates that a higher diurnal PA among older

adults during the daytime (11 am-4 pm) is associated with an increased survival probability, even after adjusting for age, complimenting the findings in NHANES 2003-06 (Liu et al., 2016; Cui et al., 2021). In the CGM application, the FTTM demonstrates an increased predictive capacity of baseline CGM estimated glucodensity marker compared to the traditional HbA1c biomarker in predicting time to multiple hypoglycemic events in patients with Type 1 diabetes mellitus and also captures a significant association between high maximal quantiles of CGM and lower risk of repeated Hypoglycemia.

There are multiple research directions which remain be explored based on our current research. It would be interesting to develop a formal test of goodness of fit (Fernández and Gretton, 2019; Chernozhukov et al., 2021) for the functional time transformation model based on the pseudo residuals introduced in this paper. Nonparametric tests for independence under censored or missing mechanism could also be adopted for this purpose (Matabuena et al., 2022). Another interesting direction of research might be to extend FTTM to accommodate longitudinal or multilevel functional predictors (Lin et al., 2021; Cui et al., 2022), which are becoming increasingly common with the emergence of intensive longitudinal studies in mHealth. Extending the proposed FTTM to more general classes of survival models (Gasperoni et al., 2020; Li et al., 2022) remains plausible and would be areas of future interest.

Supplementary Material

Appendix A, Supplementary Tables S1-S6 and Supplementary Figures S1-S3 are available online with this article.

Software

R software illustration of the proposed method is available with this article and will be made available on Github.

References

- Allen, N. A., J. A. Fain, B. Braun, and S. R. Chipkin (2009). Continuous glucose monitoring in non-insulin-using individuals with type 2 diabetes: acceptability, feasibility, and teaching opportunities. *Diabetes technology & therapeutics* 11(3), 151–158.
- Battelino, T., C. M. Alexander, S. A. Amiel, G. Arreaza-Rubin, R. W. Beck, R. M. Bergental, B. A. Buckingham, J. Carroll, A. Ceriello, E. Chow, et al. (2023). Continuous glucose monitoring and metrics for clinical trials: an international consensus statement. *The lancet Diabetes & endocrinology* 11(1), 42–57.
- Bigot, J., R. Gouet, T. Klein, and A. López (2018). Upper and lower risk bounds for estimating the wasserstein barycenter of random measures on the real line. *Electron. J. Statist.* 12(2), 2253–2289.
- Burge, M. R., S. Mitchell, A. Sawyer, and D. S. Schade (2008). Continuous glucose monitoring: the future of diabetes management. *Diabetes Spectrum* 21(2), 112–119.
- Chen, K., Z. Jin, and Z. Ying (2002). Semiparametric analysis of transformation models with censored data. *Biometrika* 89(3), 659–668.
- Cheng, S., L. J. Wei, and Z. Ying (1995). Analysis of transformation models with censored data. *Biometrika* 82(4), 835–845.
- Chernozhukov, V., K. Wüthrich, and Y. Zhu (2021). Distributional conformal prediction. *Proceedings of the National Academy of Sciences* 118(48), e2107794118.

- Coffman, D. L., J. J. Dziak, K. Litson, Y. Chakraborti, M. E. Piper, and R. Li (2023). A causal approach to functional mediation analysis with application to a smoking cessation intervention. *Multivariate Behavioral Research* 58(5), 859–876.
- Cui, E., C. M. Crainiceanu, and A. Leroux (2021). Additive functional cox model. *Journal of Computational and Graphical Statistics* 30(3), 780–793.
- Cui, E., A. Leroux, E. Smirnova, and C. M. Crainiceanu (2022). Fast univariate inference for longitudinal functional models. *Journal of Computational and Graphical Statistics* 31(1), 219–230.
- Eriksson, F., J. Li, T. Scheike, and M.-J. Zhang (2015). The proportional odds cumulative incidence model for competing risks. *Biometrics* 71(3), 687–695.
- Fan, Y., G. M. James, and P. Radchenko (2015). Functional additive regression. *The Annals of Statistics* 43(5), 2296–2325.
- Fernández, T. and A. Gretton (2019). A maximum-mean-discrepancy goodness-of-fit test for censored data. In *The 22nd International Conference on Artificial Intelligence and Statistics*, pp. 2966–2975. PMLR.
- Gasperoni, F., F. Ieva, A. M. Paganoni, C. H. Jackson, and L. Sharples (2020). Non-parametric frailty cox models for hierarchical time-to-event data. *Biostatistics* 21(3), 531–544.
- Gellar, J. E., E. Colantuoni, D. M. Needham, and C. M. Crainiceanu (2014). Variable-domain functional regression for modeling icu data. *Journal of the American Statistical Association* 109(508), 1425–1439.
- Gellar, J. E., E. Colantuoni, D. M. Needham, and C. M. Crainiceanu (2015). Cox regression models with functional covariates for survival data. *Statistical modelling* 15(3), 256–278.

- Ghosal, R., S. Ghosh, J. Urbanek, J. A. Schrack, and V. Zipunnikov (2023). Shape-constrained estimation in functional regression with bernstein polynomials. *Computational Statistics & Data Analysis* 178, 107614.
- Ghosal, R. and A. Maity (2023). Variable selection in nonlinear function-on-scalar regression. *Biometrics* 79(1), 292–303.
- Ghosal, R., A. Maity, T. Clark, and S. B. Longo (2020). Variable selection in functional linear concurrent regression. *Journal of the Royal Statistical Society: Series C (Applied Statistics)* 69(3), 565–587.
- Ghosal, R., M. Matabuena, and J. Zhang (2023). Functional proportional hazards mixture cure model with applications in cancer mortality in nhanes and post icu recovery. *Statistical Methods in Medical Research* 32(11), 2254–2269.
- Ghosal, R., V. R. Varma, D. Volfson, I. Hillel, J. Urbanek, J. M. Hausdorff, A. Watts, and V. Zipunnikov (2023). Distributional data analysis via quantile functions and its application to modeling digital biomarkers of gait in alzheimer’s disease. *Biostatistics* 24(3), 539–561.
- Group, J. D. R. F. C. G. M. S. (2009). The effect of continuous glucose monitoring in well-controlled type 1 diabetes. *Diabetes care* 32(8), 1378–1383.
- Harrell Jr, F. E., K. L. Lee, and D. B. Mark (1996). Multivariable prognostic models: issues in developing models, evaluating assumptions and adequacy, and measuring and reducing errors. *Statistics in medicine* 15(4), 361–387.
- Hermanns, N., L. Heinemann, G. Freckmann, D. Waldenmaier, and D. Ehrmann (2019). Impact of cgm on the management of hypoglycemia problems: overview and secondary analysis of the hypode study. *Journal of diabetes science and technology* 13(4), 636–644.

- Huang, C., P. Thompson, Y. Wang, Y. Yu, J. Zhang, D. Kong, R. R. Colen, R. C. Knickmeyer, H. Zhu, A. D. N. Initiative, et al. (2017). Fgwas: functional genome wide association analysis. *Neuroimage* 159, 107–121.
- Ikeda, T., M. Dowd, and J. L. Martin (2008). Application of functional data analysis to investigate seasonal progression with interannual variability in plankton abundance in the bay of fundy, canada. *Estuarine, Coastal and Shelf Science* 78(2), 445–455.
- John, D., Q. Tang, F. Albinali, and S. Intille (2019). An open-source monitor-independent movement summary for accelerometer data processing. *Journal for the Measurement of Physical Behaviour* 2(4), 268–281.
- Koner, S., S. Y. Park, and A.-M. Staicu (2024). Profit: projection-based test in longitudinal functional data. *Journal of Nonparametric Statistics*, 1–28.
- Kong, D., J. G. Ibrahim, E. Lee, and H. Zhu (2018). Flcrm: Functional linear cox regression model. *Biometrics* 74(1), 109–117.
- Leroux, A., J. Di, E. Smirnova, E. J. McGuffey, Q. Cao, E. Bayatmokhtari, L. Tabacu, V. Zipunnikov, J. K. Urbanek, and C. Crainiceanu (2019). Organizing and analyzing the activity data in nhanes. *Statistics in biosciences* 11(2), 262–287.
- Li, C., L. Xiao, and S. Luo (2022). Joint model for survival and multivariate sparse functional data with application to a study of alzheimer’s disease. *Biometrics* 78(2), 435–447.
- Li, Y., I. Xu, and C. Liu (2021). Functional data modeling and hypothesis testing for longitudinal alzheimer genome-wide association studies. *Modern Statistical Methods for Health Research*, 353–379.

- Lin, J., K. Li, and S. Luo (2021). Functional survival forests for multivariate longitudinal outcomes: Dynamic prediction of alzheimer’s disease progression. *Statistical methods in medical research* 30(1), 99–111.
- Liu, C., W. Su, K.-Y. Liu, G. Yin, and X. Zhao (2024). Efficient estimation for functional accelerated failure time model. *arXiv preprint arXiv:2402.05395*.
- Liu, L., Y. Shi, T. Li, Q. Qin, J. Yin, S. Pang, S. Nie, and S. Wei (2016). Leisure time physical activity and cancer risk: evaluation of the who’s recommendation based on 126 high-quality epidemiological studies. *British journal of sports medicine* 50(6), 372–378.
- Matabuena, M., P. Felix, C. Garcia-Meixide, and F. Gude (2022). Kernel machine learning methods to handle missing responses with complex predictors. application in modelling five-year glucose changes using distributional representations. *Computer Methods and Programs in Biomedicine* 221, 106905.
- Matabuena, M., M. Karas, S. Riazati, N. Caplan, and P. R. Hayes (2023). Estimating knee movement patterns of recreational runners across training sessions using multilevel functional regression models. *The American Statistician* 77(2), 169–181.
- Matabuena, M. and A. Petersen (2023). Distributional data analysis of accelerometer data from the nhanes database using nonparametric survey regression models. *Journal of the Royal Statistical Society Series C: Applied Statistics* 72(2), 294–313.
- Matabuena, M., A. Petersen, J. C. Vidal, and F. Gude (2021). Glucodensities: a new representation of glucose profiles using distributional data analysis. *Statistical Methods in Medical Research* 30(6), 1445–1464. PMID: 33760665.
- McLain, A. C. and S. K. Ghosh (2013). Efficient sieve maximum likelihood estimation of time-transformation models. *Journal of Statistical Theory and Practice* 7, 285–303.

- Östenson, C., P. Geelhoed-Duijvestijn, J. Lahtela, R. Weitgasser, M. Markert Jensen, and U. Pedersen-Bjergaard (2014). Self-reported non-severe hypoglycaemic events in europe. *Diabetic Medicine* 31(1), 92–101.
- Patel, A. V., C. M. Friedenreich, S. C. Moore, S. C. Hayes, J. K. Silver, K. L. Campbell, K. Winters-Stone, L. H. Gerber, S. M. George, J. E. Fulton, et al. (2019). American college of sports medicine roundtable report on physical activity, sedentary behavior, and cancer prevention and control. *Medicine and science in sports and exercise* 51(11), 2391.
- Petersen, A. and H.-G. Müller (2016). Functional data analysis for density functions by transformation to a hilbert space. *The Annals of Statistics* 44(1), 183–218.
- Qu, S., J.-L. Wang, and X. Wang (2016). Optimal estimation for the functional cox model. *The Annals of Statistics* 44(4), 1708–1738.
- Ramsay, J. and B. Silverman (2005). *Functional Data Analysis*. New York: Springer-Verlag.
- Scheipl, F. and S. Greven (2016). Identifiability in penalized function-on-function regression models.
- Smirnova, E., A. Leroux, Q. Cao, L. Tabacu, V. Zipunnikov, C. Crainiceanu, and J. K. Urbanek (2020). The predictive performance of objective measures of physical activity derived from accelerometry data for 5-year all-cause mortality in older adults: National health and nutritional examination survey 2003–2006. *The Journals of Gerontology: Series A* 75(9), 1779–1785.
- van Beers, C. A. and J. H. DeVries (2016). Continuous glucose monitoring: impact on hypoglycemia. *Journal of Diabetes Science and Technology* 10(6), 1251–1258.

- Wang, J. and S. K. Ghosh (2012). Shape restricted nonparametric regression with bernstein polynomials. *Computational Statistics & Data Analysis* 56(9), 2729–2741.
- Wu, P.-S. and H.-G. Müller (2010). Functional embedding for the classification of gene expression profiles. *Bioinformatics* 26(4), 509–517.
- Zeng, D. and D. Lin (2006). Efficient estimation of semiparametric transformation models for counting processes. *Biometrika* 93(3), 627–640.
- Zeng, D. and D. Lin (2007). Semiparametric transformation models with random effects for recurrent events. *Journal of the American Statistical Association* 102(477), 167–180.
- Zipunnikov, V., B. Caffo, D. M. Yousem, C. Davatzikos, B. S. Schwartz, and C. Crainiceanu (2011). Functional principal component model for high-dimensional brain imaging. *NeuroImage* 58(3), 772–784.
- Zipunnikov, V., S. Greven, H. Shou, B. Caffo, D. S. Reich, and C. Crainiceanu (2014). Longitudinal high-dimensional principal components analysis with application to diffusion tensor imaging of multiple sclerosis. *The annals of applied statistics* 8(4), 2175.

Supplementary Material for Functional Time Transformation Models with Applications to Wearable Data

Rahul Ghosal¹, Marcos Matabuena², Sujit K. Ghosh³

¹ Department of Epidemiology and Biostatistics, University of South Carolina

²Department of Biostatistics, Harvard University, Boston, MA 02115, USA

³ Department of Statistics, North Carolina State University

July 1, 2024

arXiv:2406.19716v1 [stat.ME] 28 Jun 2024

1 Appendix A: Consistency of the Estimators

We assume the following regularity conditions in order to establish consistency of the estimators:

- I. The true transformation function $H_0(\cdot)$ is increasing and bounded over $(0, \tau]$.
- II. Conditional on $\mathbf{X}, X_f(\cdot)$ the survival time T is independent of C , and $S_C(\cdot | \mathbf{X}, X_f(\cdot))$ is ancillary for $(\boldsymbol{\beta}, \beta(\cdot), H)$.
- III. For $r = 1, 2$ the r th derivative of $H_0(\cdot)$ exists, is bounded and continuous on $(0, \tau]$, and $\boldsymbol{\beta}$ lies in the interior of a compact set $B \subseteq \mathbb{R}^p$.
- IV. The coefficient function $\beta(\cdot) \in \mathcal{K} \subset \mathcal{L}^2[0, 1]$, where \mathcal{K} is compact and for $r = 1, 2$ the r th derivative of $\beta_0(\cdot)$ exists and is in $\mathcal{L}^2[0, 1]$.
- V. \mathbf{X} is bounded. $\exists M_1 > 0$ such that $\Pr(\|\mathbf{X}\| \leq M_1) = 1$, where $\|\cdot\|$ denotes the Euclidean norm in \mathbb{R}^p .
- VI. $\exists M_2 > 0$ s.t $\Pr(\sup_{s \in [0, 1]} |X_f(s)| \leq M_2) = 1$.
- VII. The c.d.f. of the error distribution F_ϵ is defined on \mathbb{R} and has first, and second derivatives that are continuous and bounded. Furthermore, $f_\epsilon(t)$ and $\bar{F}_\epsilon(t)$ are log-concave in t .
- VIII. The distribution function of the censoring values $F_C(\cdot | \mathbf{X}, X_f(\cdot))$ has first and second derivatives that are continuous and bounded on $(0, \tau]$. Furthermore, the bounds do not depend on $\mathbf{X}, X_f(\cdot)$.
- IX. Let $N_n = \max_{\ell \in \{0, 1\}} N_\ell$, and we have $N_n = O(n^\kappa)$, where $0 < \kappa < 1$.

Define the metric d as,

$$d\{(\boldsymbol{\beta}_1, \beta_1(\cdot), H_1), (\boldsymbol{\beta}_2, \beta_2(\cdot), H_2)\} = \|\boldsymbol{\beta}_1 - \boldsymbol{\beta}_2\| + \|\beta_1(\cdot) - \beta_2(\cdot)\|_{\mathcal{H}} + \|H_1 - H_2\|_{F_Y},$$

where $\|H_1 - H_2\|_{F_Y} = \int \{H_1(t) - H_2(t)\}^2 dF_Y(t)$, with $F_Y(t) = \Pr(T \wedge C \leq t)$ and $\|\beta_1(\cdot) - \beta_2(\cdot)\|_{\mathcal{H}} = (\int_0^1 \{\beta_1(s) - \beta_2(s)\}^2 ds)^{1/2}$.

Theorem S1 *Suppose that assumptions (I)-(IX) hold. Then*

$$d \left\{ \left(\hat{\boldsymbol{\beta}}_{n, N_0, N_1}, \hat{\beta}(\cdot)_{n, N_1}, \hat{H}_{N_0} \right), (\boldsymbol{\beta}_0, \beta_0(\cdot), H_0) \right\} \rightarrow 0$$

almost surely, as $n \rightarrow \infty$.

Proof: The proof follows the steps of Theorem 1 in [McLain and Ghosh \(2013\)](#) and is based on Theorem 3.1 of [Wang \(1985\)](#) on results for consistency of approximate maximum likelihood estimators. Note that $\hat{\phi}_{N_0, N_1} = \hat{\phi}_{\mathbf{N}} = \left(\hat{\boldsymbol{\beta}}_{n, N_0, N_1}, \hat{\beta}(\cdot)_{n, N_1}, \hat{H}_{N_0} \right)$ maximizes the log-likelihood $l_n(\boldsymbol{\beta}, \gamma, \boldsymbol{\theta} | \mathbf{X}, X_f(\cdot), \mathbf{Y})$ in equation (10) of the paper and is an approximate maximum likelihood estimator based on the Bernstein-Weierstrass approximation theorem ([Lorentz, 2013](#)). Since, $N_n = O(n^\kappa)$, the rate at which N_0, N_1 increase must be such that $N_\ell \rightarrow \infty$ and $N_\ell/n \rightarrow 0$ as $n \rightarrow \infty$ ($\ell = 0, 1$) and $\hat{\phi}_{\mathbf{N}}$ maximizes the log-likelihood as $N_0, N_1 \rightarrow \infty$.

It is enough to show that ([McLain and Ghosh, 2013](#)) (suppressing the dependence of $\hat{\boldsymbol{\beta}}$ and $\hat{\beta}(s)$ on N_0, N_1)

$$\int_{-\infty}^{\infty} \left| F_\epsilon \left\{ \hat{H}_{N_0}(u) + \hat{\boldsymbol{\beta}}^T \mathbf{X} + \int_0^1 X_f(s) \hat{\beta}(s) ds \right\} - F_\epsilon \left\{ H_0(u) + \boldsymbol{\beta}^T \mathbf{X} + \int_0^1 X_f(s) \beta(s) ds \right\} \right| dF_Y(u | \mathbf{X}, X_f(\cdot)) \rightarrow 0, \quad (1)$$

almost surely as $n \rightarrow \infty$. Theorem S1 then follows from the boundedness of the transformation function $H_0(\cdot)$ on $(0, \tau]$, the boundedness of $X_f(s)$, the continuity of the error c.d.f. F_ϵ , and the dominated convergence theorem.

To show condition (1) we verify the five required assumptions of Theorem 3.1 in [Wang \(1985\)](#). Let us define $\pi \left(\hat{\phi}_{\mathbf{N}}, t, \mathbf{X}, X_f(\cdot) \right) = F_\epsilon \left\{ \hat{H}_{N_0}(t) + \hat{\boldsymbol{\beta}}^T \mathbf{X} + \int_0^1 X_f(s) \hat{\beta}(s) ds \right\}$, with $\pi(\phi_0, t, \mathbf{X}, X_f(\cdot)) = F_T(t | \mathbf{X}, X_f(\cdot))$ (see equation (2) of the paper).

The assumption (i) in [Wang \(1985\)](#) is satisfied based on the definition of our metric, the assumption that B is a bounded subset of \mathbb{R}^p and since $\beta(\cdot) \in \mathcal{K} \subset \mathcal{L}^2[0, 1]$. Denote $\Phi = B \times \mathcal{K} \times \mathcal{F}$. Then (Φ, d) is a separable compact metric space. Define $V_b(\phi_0)$, $b \geq 1$ as a decreasing sequence of basic neighborhoods of $\pi(\phi_0, t, \mathbf{X}, X_f(\cdot))$ with radius b^{-1} . Let us also define $A_\varphi(\phi)$ as: $A_\varphi(\phi) = \varphi \pi(\phi, t, \mathbf{X}, X_f(\cdot)) + (1 - \varphi) \pi(\phi_0, t, \mathbf{X}, X_f(\cdot))$.

Denote the observed data for subject i as $\mathbf{Z}_i = (Y_i, \Delta_i, \mathbf{X}_i, X_{fi}(\cdot))$. For all $\phi \in \Phi$, let $l\{\mathbf{Z}, A_\varphi(\phi)\} = \Delta_i \log \{A'_\varphi(\phi)\} + (1 - \Delta_i) \log \{A_\varphi(\phi)\}$ with $A'_\varphi(\phi) = \partial A_\varphi(\phi) / \partial t$. Note that for every $b \geq 1$ there exists a $\varphi \in (0, 1]$ with $\varphi \leq b^{-1}$ such that $A_\varphi(\phi) \in V_b(\phi_0)$.

Under assumptions V and VI, to verify conditions (ii) and (iii) in Wang (1985) it is enough to show that (define $0/0 \equiv 0$)

$$E_{(Y,\Delta)} [l\{\mathbf{Z}, A_\varphi(\phi)\} / l(\mathbf{Z}, \phi) \mid \mathbf{X}, X_f(\cdot)] > 0, \quad (2)$$

The marginal density of Y is given by

$$f_Y(y \mid \mathbf{X}, X_f(\cdot)) = S_C(y)f_T(y \mid \mathbf{X}, X_f(\cdot)) + S_T(y)f_C(y \mid \mathbf{X}, X_f(\cdot)).$$

Denoting $\pi' = (\partial/\partial t)\pi$, and using $\pi(\phi_0, t, \mathbf{X}, X_f(\cdot)) = F_T(t \mid \mathbf{X}, X_f(\cdot))$, we have,

$$\begin{aligned} \int \frac{\pi'(\phi, u, \mathbf{X}, X_f(\cdot))}{\pi'(\phi_0, u, \mathbf{X}, X_f(\cdot))} S_C(u)f_T(u \mid \mathbf{X}, X_f(\cdot))du &= \int \pi'(\phi, u, \mathbf{X}, X_f(\cdot))S_C(u)du \\ &< \int \pi'(\phi, u, \mathbf{X}, X_f(\cdot))du \leq 1. \end{aligned}$$

and

$$\int \frac{\pi(\phi, u, \mathbf{X}, X_f(\cdot))}{\pi(\phi_0, u, \mathbf{X}, X_f(\cdot))} S_T(u)f_C(u \mid \mathbf{X}, X_f(\cdot))du = \int \pi(\phi, u, \mathbf{X}, X_f(\cdot))f_C(u)du < \int f_C(u)du = 1.$$

Applying Jensen's inequality, we have

$$\int \log \left\{ \frac{\pi'(\phi, u, \mathbf{X}, X_f(\cdot))}{\pi'(\phi_0, u, \mathbf{X}, X_f(\cdot))} \right\} S_C(u)f_T(u \mid \mathbf{X}, X_f(\cdot))du < 0. \quad (3)$$

and

$$\int \log \left\{ \frac{\pi(\phi, u, \mathbf{X}, X_f(\cdot))}{\pi(\phi_0, u, \mathbf{X}, X_f(\cdot))} \right\} S_T(u)f_C(u \mid \mathbf{X}, X_f(\cdot))du < 0. \quad (4)$$

Hence based on (3) we have,

$$\begin{aligned} E_Y \left[\frac{l(Y, 1, \mathbf{X}, X_f(\cdot), A_\varphi(\phi))}{l\{Y, 1, \mathbf{X}, X_f(\cdot), \phi\}} \mid \mathbf{X}, X_f(\cdot), \Delta = 1 \right] &= E_Y \left[\log \left\{ \frac{A_\varphi(\phi)}{\pi'(\phi, Y, \mathbf{X}, X_f(\cdot))} \right\} \mid \mathbf{X}, X_f(\cdot), \Delta = 1 \right] \\ &\geq E_Y \left[\log \left\{ \frac{\pi'(\theta_0, Y, \mathbf{X}, X_f(\cdot))}{\pi'(\theta, Y, \mathbf{X}, X_f(\cdot))} \right\} \mid \mathbf{X}, X_f(\cdot), \Delta = 1 \right] \\ &> 0, \end{aligned}$$

and similar result for $\Delta = 0$ using (4). This verifies the condition (2). The last two conditions (iv) and (v) of Wang (1985) are easily verified by the continuity of $l\{\mathbf{Z}, \phi\}$ and this proves the Theorem S1.

2 Appendix B: Supplementary Tables

Table S1: Estimated coverage from the 95% Wald confidence intervals for the functional and scalar coefficients, Scenario A1. For the functional coefficients the average of the point-wise coverage over S (grid of length $m = 101$ on $\mathcal{S} = [0, 1]$) is reported.

| Sample Size | $\beta(s)$ | β_1 | β_2 |
|-------------|------------|-----------|-----------|
| $n = 100$ | 0.95 | 0.93 | 0.93 |
| $n = 300$ | 0.97 | 0.92 | 0.94 |
| $n = 500$ | 0.93 | 0.92 | 0.95 |

Table S2: Estimated coverage from the 95% Wald confidence intervals for the functional and scalar coefficients, Scenario A2. For the functional coefficients the average of the point-wise coverage over S (grid of length $m = 101$ on $\mathcal{S} = [0, 1]$) is reported.

| Sample Size | $\beta(s)$ | β_1 | β_2 |
|-------------|------------|-----------|-----------|
| $n = 100$ | 0.94 | 0.93 | 0.95 |
| $n = 300$ | 0.92 | 0.95 | 0.93 |
| $n = 500$ | 0.97 | 0.96 | 0.98 |

Table S3: Descriptive Statistics of the Sample considered in the NHNAES 2011-2014 application. The mean (standard deviation) and count (percentage) is presented for continuous and categorical variables respectively.

| Variable | Total (n=3032) | Deceased (n=582) | Survivors (n=2450) | p-value |
|----------|----------------|------------------|--------------------|---------|
| Age | 66.0 (9.36) | 72.31 (8.80) | 64.50 (8.85) | < 0.001 |
| Gender | | | | < 0.001 |
| Female | 1687 (55.6) | 278 (47.8) | 1409 (57.5) | |
| Male | 1345 (44.4) | 304 (52.2) | 1041 (42.5) | |
| BMI | 30.06 (7.07) | 28.89 (7.35) | 30.34 (6.98) | < 0.001 |

Table S4: Estimated Scalar coefficients from the FTTM method along with their 95% confidence intervals in the NHANES application.

| Variable | Estimate (CI) |
|-----------------|-----------------------|
| Age | 0.077 (0.015,0.139) |
| Gender (Female) | -0.129 (-0.457,0.198) |
| BMI | -0.024 (-0.070,0.022) |

Table S5: Descriptive Statistics of the Sample considered in the CGM application. Adverse Event is defined as having 65 episodes of hypoglycemia during followup. The mean (standard deviation) and count (percentage) is presented for continuous and categorical variables respectively.

| Variable | Total (n=296) | Adverse Event (n=266) | No Adverse event (n=30) | p-value |
|----------|---------------|-----------------------|-------------------------|---------|
| Age | 22.92 (14.68) | 23.5 (14.83) | 17.9 (12.35) | 0.048 |
| Gender | | | | 0.43 |
| Female | 163 (55.1) | 149 (56.0) | 14 (46.67) | |
| Male | 133 (44.9) | 117 (44.0) | 16 (53.33) | |
| HbA1C | 7.91 (0.64) | 7.87 (0.61) | 8.29 (0.77) | < 0.001 |

Table S6: Estimated Scalar coefficients from the FTTM method along with their 95% confidence intervals in the CGM application.

| Variable | Estimate (CI) |
|---------------|----------------------|
| Age | 0.009 (-0.027,0.046) |
| Gender (Male) | -0.492 (-1.22,0.239) |

3 Appendix C: Supplementary Figures

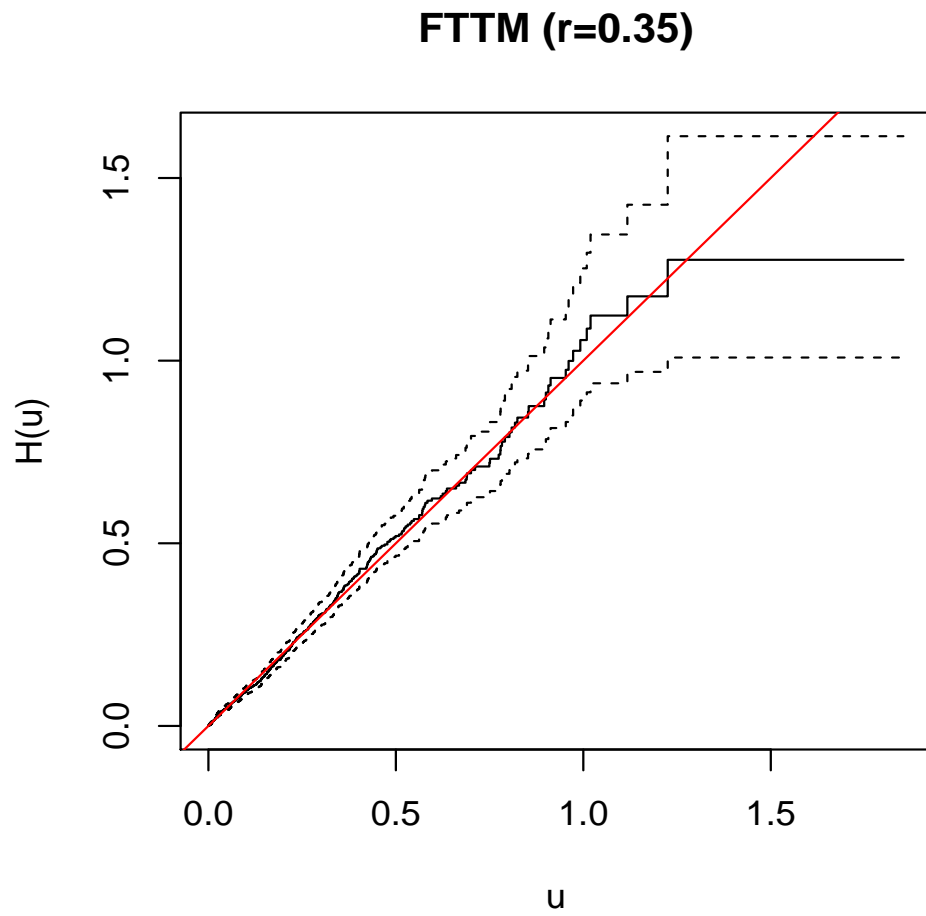


Figure S1: Nelson-Allen estimate of cumulative hazard $\hat{\Lambda}(u)$ (solid line) and the associated 95% confidence interval based on the fitted FTTM pseudo residuals U_i for the NHANES 2011-2014 application.

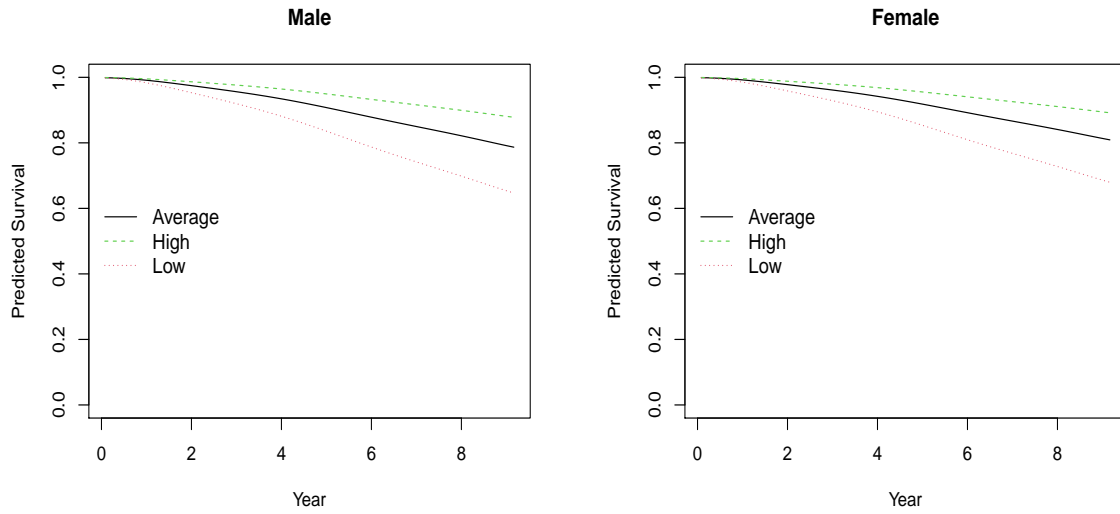


Figure S2: Predicted survival probabilities from the FTTM for Male and Female participants with Age=66, BMI=30.06 and diurnal PA belonging to one of Average, High or Low group in the NHANES application.

FTTM (r=4)

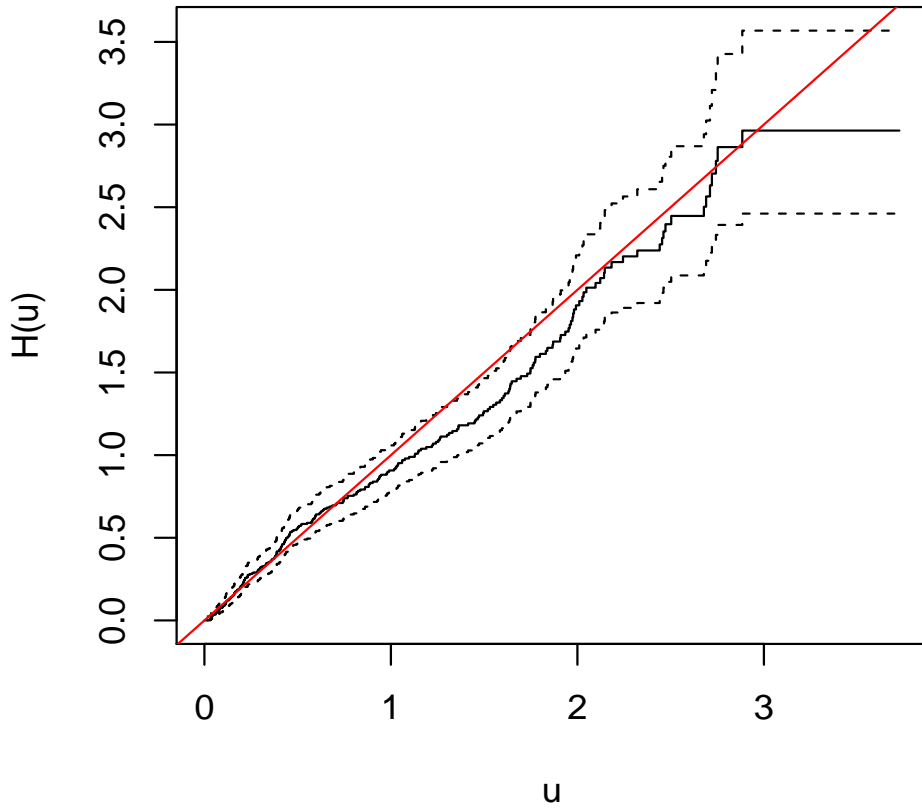


Figure S3: Nelson Allen estimate of cumulative hazard $\hat{\Lambda}(u)$ (solid line) and the associated 95% confidence interval based on the fitted FTTM pseudo residuals U_i for the CGM application.

References

- Lorentz, G. G. (2013). *Bernstein polynomials*. American Mathematical Soc.
- McLain, A. C. and S. K. Ghosh (2013). Efficient sieve maximum likelihood estimation of time-transformation models. *Journal of Statistical Theory and Practice* 7, 285–303.
- Wang, J.-L. (1985). Strong consistency of approximate maximum likelihood estimators with applications in nonparametrics. *The Annals of Statistics*, 932–946.